Wind and Structures, *Vol. 28, No. 3 (2019) 171-180*
DOI: https://doi.org/10.12989/was.2019.28.3.171

An iterative approach for time-domain flutter analysis of bridges based on restart technique

Wen-ming Zhang[*1], Kai-rui Qian[1a], Lian Xie[2b] and Yao-jun Ge[3c]

[1]*Key Laboratory of Concrete and Prestressed Concrete Structures of the Ministry of Education, Southeast University, Nanjing 211189, P.R. China*
[2]*T. Y. Lin International Engineering Consulting (China) Co., Ltd, Chongqing 401121, P.R. China*
[3]*State Key Lab for Disaster Reduction in Civil Engineering, Tongji University, Shanghai 200092, P.R. China*

(Received March 7, 2018, Revised July 17, 2018, Accepted September 7, 2018)

Abstract. This paper presents a restart iterative approach for time-domain flutter analysis of long-span bridges using the commercial FE package ANSYS. This approach utilizes the recursive formats of impulse-response-function expressions for bridge's aeroelastic forces. Nonlinear dynamic equilibrium equations are iteratively solved by using the restart technique in ANSYS, which enable the equilibrium state of system to get back to last moment absolutely during iterations. The condition for the onset of flutter instability becomes that, at a certain wind velocity, the amplitude of vibration is invariant with time. A long-span suspension bridge was taken as a numerical example to verify the applicability and accuracy of the proposed method by comparing calculated results with wind tunnel tests. The proposed method enables the bridge designers and engineering practitioners to carry out time-domain flutter analysis of bridges in commercial FE package ANSYS.

Keywords: long-span bridge; flutter; time domain; aeroelastic force; finite element (FE) model; ANSYS

1. Introduction

With the ever-growing span being employed, long-span bridges become more and more soft and light. As a result, wind resistance of bridge structures is faced with unprecedented challenges. One of the most important aerodynamic characteristics is flutter instability, which takes place when a bridge is exposed to wind speeds above a certain critical value.

Two different analytical methods, namely frequency domain and time domain, are commonly adopted to study the flutter of long-span cable-supported bridge structures (Caracoglia and Jones 2003, Ge and Tanaka 2000). The frequency-domain analysis method is simple to use, yet it still belongs to the linear analysis category. The time-domain analysis can consider nonlinear characteristics of structure and reflect the changing trend of time history of structural self-excited vibration, thus this method presents the vibration motion and amplitude of variation of bridge structures more accurately. Time-domain expressions of self-excited force are needed in the time-domain solution. At present there are two major time-domain expressions of bridge self-excited force. First is the combination of step function and aerodynamic derivatives of bridge deck (Caracoglia and Jones 2003, Ding *et al* 2002, Ge and Tanaka 2000), which can be directly applied in time-domain calculation. However, when aerodynamic coupling is taken into consideration, the step function of aerodynamic force is difficult to determine. The second is the combination of impulse response function and rational function (Li and Lin 1995, Lin and Li 1993), in which, according to the relations between aerodynamic derivatives and reduced wind velocity, the self-excited force of structure can be calculated directly from transfer function for unsteady aerodynamic force of bridge deck after certain parameter fitting.

As for the frequency domain analysis, the multimode approach (Agar 1989, Namini *et al.* 1992, Tanaka *et al.* 1992, Katsuchi *et al.* 1998, 1999, and Ding *et al*. 2002) and the full-mode approach (Miyata and Yamada 1990, Dung *et al.* 1998, Ge and Tanaka 2000, Ding *et al.* 2002) are two general methods commonly used at present. Currently, these two approaches have been incorporated into the commercial FE package ANSYS (Hua and Chen 2008), making it is more convenient to carry out flutter analysis in frequency domain. The specific user-defined element *Matrix27* is commonly employed in ANSYS to model the aerodynamic forces acting on the structure when calculating the self-excited vibration response of bridge (Hua *et al.* 2007, Hua and Chen 2008, Yang *et al*. 2011, Zhang *et al.* 2011, Wang *et al.* 2014b, Han *et al.* 2015a, b, Tang *et al.* 2018).

However, the *Matrix27*-based way to model self-excited force is not suitable for time-domain flutter analysis. The element *Matrix27* requires the input of structural frequency under different wind velocities, meaning that the estimation of frequency of bridge structure should be done in advance, which might cause an estimation frequency error. Moreover, human intervention is needed during this calculating process. Therefore, ANSYS-based approach for time-domain flutter analysis is seldom reported.

In time-domain buffeting analysis, the *Matrix27*-based

*Corresponding author, Associate Professor
E-mail: zwm@seu.edu.cn
[a] Master Degree Candidate
[b] Master
[c] Ph.D., Professor

ISSN: 1226-6116 (Print), 1598-6225 (Online)

way to model self-excited force has been adopted (Chen *et al.* 2009, Wang, *et al.* 2014a). Due to the frequency input, the calculating method of element *Matrix27* can only provide a relatively accurate reflection on the self-excited vibration response of structure under tracking mode, instead of an accurate reflection on multi-mode coupling of structure. Therefore, using this method to calculate structure buffeting would cause significant calculating error of self-exited vibration response. As a summary, an alternative way to simulate self-excited force in ANSYS is necessary.

Based on the impulse function expressions of self-excited force (Li and Lin 1995, Lin and Li 1993), the self-excited force of structure can be directly acted on specific nodes of structure as concentrated force and the response signal of structural time histories can be calculated without estimating structure frequency in advance. The signal can then be transformed to structural vibration frequency via Fourier transform, thereby leading to an accurate reflection of all participating modes and making the calculating results more reliable. The authors want to incorporate the impulse function expressions of self-excited force into the ANSYS.

This paper raises a restart iterative method by using ANSYS to carry out time-domain analysis of self-excited vibration response of bridge structures based on the impulse function expressions of self-excited force in time domain. This method directly puts the self-excited force as concentrated force on specific nodes of structure, iteratively calculates the vibration response at each time step by using the restart technique of ANSYS, then obtains the time-history response of bridge's self-excited vibration, and identifies the flutter critical wind velocity and flutter frequency. A suspension bridge with flat steel box girder and three pylons was used to verify the applicability and accuracy of the proposed method.

2. Expressions for impulse function of self-excited forces

The self-excited forces acting on per unit span of bridge deck can be expressed utilizing flutter derivatives put forward by Scanlan (1978) and Jain *et al.* (1996)

$$\begin{aligned}
L_{se}(t) &= \frac{1}{2}\rho U^2(2B)\left(KH_1^*\frac{\dot{h}}{U}+KH_2^*\frac{B\dot{\alpha}}{U}+K^2H_3^*\alpha\right.\\
&\left.+K^2H_4^*\frac{h}{B}+KH_5^*\frac{\dot{p}}{U}+K^2H_6^*\frac{p}{B}\right)\\
D_{se}(t) &= \frac{1}{2}\rho U^2(2B)\left(KP_1^*\frac{\dot{p}}{U}+KP_2^*\frac{B\dot{\alpha}}{U}+K^2P_3^*\alpha\right.\\
&\left.+K^2P_4^*\frac{p}{B}+KP_5^*\frac{\dot{h}}{U}+K^2P_6^*\frac{h}{B}\right)\\
M_{se}(t) &= \frac{1}{2}\rho U^2(2B^2)\left(KA_1^*\frac{\dot{h}}{U}+KA_2^*\frac{B\dot{\alpha}}{U}+K^2A_3^*\alpha\right.\\
&\left.+K^2A_4^*\frac{h}{B}+KA_5^*\frac{\dot{p}}{U}+K^2A_6^*\frac{p}{B}\right)
\end{aligned} \tag{1}$$

where L_{se}, D_{se} and M_{se} are motion-induced aerodynamic lift force, drag force and pitching moment, respectively; ρ is air mass density; U is wind velocity; B is deck width; $K=\omega B/U$ is reduced frequency (ω refers to natural circular frequency of bridge); H_i^*, P_i^* and A_i^*(i=1~6) are frequency dependent flutter derivatives; h, p and α are the vertical, lateral and torsional displacements, respectively; each dot denotes the differentiation with respect to time t.

Eq. (1) is the real-number expression for self-excited forces of bridge deck, which can also be presented in form of complex notation (Starossek 1998)

$$\begin{aligned}
L_{se}(t) &= \omega^2\rho B^2\left[C_{Lh}(v)h(t)+C_{Lp}(v)p(t)+C_{L\alpha}(v)\alpha(t)\right]\\
D_{se}(t) &= \omega^2\rho B^2\left[C_{Dh}(v)h(t)+C_{Dp}(v)p(t)+C_{D\alpha}(v)\alpha(t)\right]\\
M_{se}(t) &= \omega^2\rho B^2\left[BC_{Mh}(v)h(t)+BC_{Mp}(v)p(t)\right.\\
&\left.+B^2C_{M\alpha}(v)\alpha(t)\right]
\end{aligned} \tag{2}$$

where $v=2\pi/K$ is reduced wind velocity; C_{rs} (r=D, L, M; s=h, p, α) are complex self-excitation coefficients, and their relations with flutter derivatives in Eq. (1) are as follows

$$\left.\begin{aligned}
&C_{Lh}=H_4^*+iH_1^*,\ C_{Lp}=H_6^*+iH_5^*, C_{L\alpha}=H_3^*+iH_2^*\\
&C_{Dh}=P_6^*+iP_5^*,\ \ C_{Dp}=P_4^*+iP_1^*, C_{D\alpha}=P_3^*+iP_2^*\\
&C_{Mh}=A_4^*+iA_1^*,\ \ C_{Mp}=A_6^*+iA_5^*, C_{M\alpha}=A_3^*+iA_2^*
\end{aligned}\right\} \tag{3}$$

where $i=\sqrt{-1}$ is imaginary unit.

Lin (1993) and Li (1995) came up with time-domain expressions for self-excited force of bridge deck through the concept of impulse response function, and Ding (2001) made the extension by including vertical, lateral, and torsional degrees of freedom:

$$\left.\begin{aligned}
&L_{se}(t)=L_h(t)+L_p(t)+L_\alpha(t)=\int_{-\infty}^{t}f_{Lh}(t-\tau)h(\tau)\mathrm{d}\tau\\
&+\int_{-\infty}^{t}f_{Lp}(t-\tau)p(\tau)\mathrm{d}\tau+\int_{-\infty}^{t}f_{L\alpha}(t-\tau)\alpha(\tau)\mathrm{d}\tau\\
&D_{se}(t)=D_h(t)+D_p(t)+D_\alpha(t)=\int_{-\infty}^{t}f_{Dh}(t-\tau)h(\tau)\mathrm{d}\tau\\
&+\int_{-\infty}^{t}f_{Dp}(t-\tau)p(\tau)\mathrm{d}\tau+\int_{-\infty}^{t}f_{D\alpha}(t-\tau)\alpha(\tau)\mathrm{d}\tau\\
&M_{se}(t)=M_h(t)+M_p(t)+M_\alpha(t)=\int_{-\infty}^{t}f_{Mh}(t-\tau)h(\tau)\mathrm{d}\tau\\
&+\int_{-\infty}^{t}f_{Mp}(t-\tau)p(\tau)\mathrm{d}\tau+\int_{-\infty}^{t}f_{M\alpha}(t-\tau)\alpha(\tau)\mathrm{d}\tau
\end{aligned}\right\} \tag{4}$$

where L_s, D_s, M_s (s=h, p, α) are components of the aerodynamic lift force, drag force and pitching moment, respectively; f_{rs} (r=L, D, M; s=h, p, α) are impulse response functions.

By taking the Fourier transform of Eqs. (2) and (4), respectively, it can be obtained that

$$\left.\begin{aligned}
L_{se}(\omega) &= \omega^2\rho B^2\left[C_{Lh}(v)h(\omega)+C_{Lp}(v)p(\omega)\right.\\
&\left.+BC_{L\alpha}(v)\alpha(\omega)\right]\\
D_{se}(\omega) &= \omega^2\rho B^2\left[C_{Dh}(v)h(\omega)+C_{Dp}(v)p(\omega)\right.\\
&\left.+BC_{D\alpha}(v)\alpha(\omega)\right]\\
M_{se}(\omega) &= \omega^2\rho B^2\left[BC_{Mh}(v)h(\omega)+BC_{Mp}(v)p(\omega)\right.\\
&\left.+B^2C_{M\alpha}(v)\alpha(\omega)\right]
\end{aligned}\right\} \tag{5}$$

$$\left.\begin{aligned} L_{se}(\omega) &= L_h(\omega)+L_p(\omega)+L_\alpha(\omega)\\ &= F_{Lh}(\omega)h(\omega)+F_{Lp}(\omega)p(\omega)+F_{L\alpha}(\omega)\alpha(\omega)\\ D_{se}(\omega) &= D_h(\omega)+D_p(\omega)+D_\alpha(\omega)\\ &= F_{Dh}(\omega)h(\omega)+F_{Dp}(\omega)p(\omega)+F_{D\alpha}(\omega)\alpha(\omega)\\ M_{se}(\omega) &= M_h(\omega)+M_p(\omega)+M_\alpha(\omega)\\ &= F_{Mh}(\omega)h(\omega)+F_{Mp}(\omega)p(\omega)+F_{M\alpha}(\omega)\alpha(\omega) \end{aligned}\right\} \quad (6)$$

where F_{rs} (r=L, D, M; s=h, p, α) refer to transfer functions between the state of motion and corresponding self-excited force. By substituting Eq. (3) into Eq. (5) and then comparing with Eq. (6), all expressions of transfer function could be obtained (Li and Lin 1995)

$$\left.\begin{aligned} F_{Lh}(\omega) &= \rho B^2\omega^2\left[H_4^*(\nu)+iH_1^*(\nu)\right]\\ F_{Lp}(\omega) &= \rho B^2\omega^2\left[H_6^*(\nu)+iH_5^*(\nu)\right]\\ F_{L\alpha}(\omega) &= \rho B^2\omega^2\left[H_3^*(\nu)+iH_2^*(\nu)\right]\\ F_{Dh}(\omega) &= \rho B^2\omega^2\left[P_6^*(\nu)+iP_5^*(\nu)\right]\\ F_{Dp}(\omega) &= \rho B^2\omega^2\left[P_4^*(\nu)+iP_1^*(\nu)\right]\\ F_{D\alpha}(\omega) &= \rho B^2\omega^2\left[P_3^*(\nu)+iP_2^*(\nu)\right]\\ F_{Mh}(\omega) &= \rho B^2\omega^2\left[A_4^*(\nu)+iA_1^*(\nu)\right]\\ F_{Mp}(\omega) &= \rho B^2\omega^2\left[A_6^*(\nu)+iA_5^*(\nu)\right]\\ F_{M\alpha}(\omega) &= \rho B^2\omega^2\left[A_3^*(\nu)+iA_2^*(\nu)\right] \end{aligned}\right\} \quad (7)$$

Lin (1993) and Li (1995) applied approximate expressions of rational function developed by Roger for unsteady aerodynamic frequency response function to bridges, and obtained the approximate expression for unsteady aerodynamic transfer function of bridge deck (taking $F_{M\alpha}$ as an example)

$$F_{M\alpha}(\omega)=\rho B^2U^2\left(C_1+iC_2\frac{B\omega}{U}+\sum_{k=3}^{4}C_k\frac{i\omega}{d_kU/B+i\omega}\right) \quad (8)$$

Let vector $\mathbf{C}_{M\alpha}$=[C_1, C_2, C_3, C_4, d_3, d_4], and all six elements are dimensionless undetermined coefficients, which are obtained by relevant fitting of flutter derivatives and reduced wind velocity, as shown in Eq. (11). The d_3 and d_4 are larger than zero. In Eq. (8), the first term represents the self-excited force induced by displacement. The second term is the self-excited force induced by velocity. The third term represents the unsteady components of aerodynamic force that lag the structure motion, which indicates the memory effect of self-excited force on structure motion and is reflected as the phase difference between self-excited force and structure motion. The number of unsteady item in Eq. (8) is 2. The rest eight transfer functions are similar to Eq. (8). With the reduced wind velocity of ν=$2\pi U/\omega B$, we can get ω=$2\pi U/\nu B$ and U=$\omega\nu B/2\pi$, and then substitute them into Eq. (8), we obtain

$$F_{M\alpha}(\nu)=\frac{\rho B^4\omega^2\nu^2}{4\pi^2}\left(C_1+iC_2\frac{2\pi}{\nu}+\sum_{k=3}^{4}C_k\frac{4\pi^2+i2\pi d_k\nu}{d_k^2\nu^2+4\pi^2}\right) \quad (9)$$

Eq. (9) is equivalent to the last transfer function in Eq. (7), thus

$$\begin{aligned} &C_1+i\frac{2\pi C_2}{\nu}+\sum_{k=3}^{4}C_k\frac{4\pi^2+i2\pi d_k\nu}{d_k^2\nu^2+4\pi^2}\\ &=\frac{4\pi^2}{\nu^2}\left[A_3^*(\nu)+iA_2^*(\nu)\right] \end{aligned} \quad (10)$$

Based on the principle that the real and imaginary parts of complex number are equivalent respectively, the fitting equations of vector $\mathbf{C}_{M\alpha}$ can be written as

$$\left.\begin{aligned} \frac{\nu}{2\pi}\left(C_2+\sum_{k=3}^{4}\frac{C_kd_k\nu^2}{d_k^2\nu^2+4\pi^2}\right) &= A_2^*(\nu)\\ \nu^2\left(\frac{C_1}{4\pi^2}+\sum_{k=3}^{4}\frac{C_k}{d_k^2\nu^2+4\pi^2}\right) &= A_3^*(\nu) \end{aligned}\right\} \quad (11)$$

In order to get vector $\mathbf{C}_{M\alpha}$, the transfer coefficient of transfer function $F_{M\alpha}$, nonlinear equations fitting for Eq. (11) is necessary yet difficult to achieve in reality. Therefore, the weighted least-square method is adopted to convert Eq. (11) into nonlinear fitting of single function, namely to solve the corresponding coefficient vector of the minimum value in Eq. (12).

$$\begin{aligned} G(\mathbf{C}_{M\alpha}) &= \sum_{i=1}^{n}w_1^2\left[A_2^*(\nu_i)-J(\nu_i,\mathbf{C}_{M\alpha1})\right]^2\\ &+\sum_{i=1}^{n}w_2^2\left[A_3^*(\nu_i)-J(\nu_i,\mathbf{C}_{M\alpha2})\right]^2 \end{aligned} \quad (12)$$

where w_1 and w_2 are weighting factors; n refers to the number of flutter derivatives corresponding to reduced velocity ν; $J(\nu_i,\mathbf{C}_{M\alpha1})$ and $J(\nu_i,\mathbf{C}_{M\alpha2})$ are fitting functions corresponding to the terms in Eq. (11) on the left side. In actual calculation, the undetermined coefficients of the transfer function with no flutter derivative data are set to zero. The fitting of the rest eight transfer functions is identical to that of $F_{M\alpha}$.

Transforming Eq. (8) through Fourier and comparing with Eqs. (4) and (6), we obtain the pitching moment induced by torsional movement corresponding to the terms in Eq. (4) on the right side.

$$\begin{aligned} M_\alpha(t) &= \rho B^2U^2\left\{C_1\alpha(t)+\frac{C_2B}{U}\dot\alpha(t)\right.\\ &\left.+\sum_{k=3}^{4}C_k\int_{-\infty}^{t}\exp\left[-\frac{d_kU}{B}(t-\tau)\right]\dot\alpha(\tau)\mathrm{d}\tau\right\} \end{aligned} \quad (13)$$

Similar to Eq. (8), the first term in the braces denotes the aerodynamic stiffness. The second term represents aerodynamic damping. The third term represents the memory effect of the history of structural movement, which is unsteady. Considering that the structure tends to be "static" when τ<0, the displacement, velocity and acceleration could be set to zero. Therefore, the lower limit

of time integral in Eq. (13) can be changed to zero, namely

$$M_\alpha(t)=\rho B^2U^2\left\{C_1\alpha(t)+\frac{C_2B}{U}\dot{\alpha}(t)+\sum_{k=3}^{4}C_k\int_0^t\exp\left[-\frac{d_kU}{B}(t-\tau)\right]\dot{\alpha}(\tau)\mathrm{d}\tau\right\} \tag{14}$$

Similarly, all component expressions for self-exited force corresponding to $L_h(t)$, $L_p(t)$, $L_\alpha(t)$, $D_h(t)$, $D_p(t)$, $D_\alpha(t)$, $M_h(t)$ and $M_p(t)$ in Eqs. (4) and (6) can be deducted following similar procedure as $M_\alpha(t)$. In order to deal with all components of self-excited force uniformly, the expression in general form is used

$$x(t)=B^2F_x(C_x,x,t) \tag{15}$$

Here

$$F_x(C_x,x,t)=\rho B^2U^2\left\{C_1x(t)+\frac{C_2B}{U}\dot{x}(t)+\sum_{k=3}^{4}C_k\int_0^t\exp\left[-\frac{d_kU}{B}(t-\tau)\right]\dot{x}(\tau)\mathrm{d}\tau\right\} \tag{16}$$

where x represents nine components respectively, namely L_h, L_p, L_α, D_h, D_p, D_α, M_h, M_p and M_α, and its displacement in corresponding direction. $\mathbf{C}_x$ refers to the six undetermined coefficients corresponding to similar component forces of $\mathbf{C}_{M\alpha}$ in Eq. (8), which is obtained by fitting Eqs. (11) and (12) and written as $\mathbf{C}_x$=[C_1, C_2, C_3, C_4, d_3, d_4]. By substituting Eq. (16) into Eq. (4), the time-domain expressions of self-excited lift force, drag force and pitching moment per unit length of bridge deck can be obtained.

$$\left.\begin{aligned}L_{se}(t)&=F_x(\mathbf{C}_{Lh},h,t)+F_x(\mathbf{C}_{Lp},p,t)+BF_x(\mathbf{C}_{L\alpha},\alpha,t)\\D_{se}(t)&=F_x(\mathbf{C}_{Dh},h,t)+F_x(\mathbf{C}_{Dp},p,t)+BF_x(\mathbf{C}_{D\alpha},\alpha,t)\\M_{se}(t)&=BF_x(\mathbf{C}_{Mh},h,t)+BF_x(\mathbf{C}_{Mp},p,t)\\&\quad+B^2F_x(\mathbf{C}_{M\alpha},\alpha,t)\end{aligned}\right\} \tag{17}$$

Eq. (17) considers the vertical, lateral, and torsional movement when calculating self-excited force, while in this paper the effect of lateral movement would not be considered.

3. The recursive format of self-excited force in time domain

As shown from Eqs. (15)- (17), the calculation of time history of self-excited forces relates to the integral of functions, therefore integration calculation is required for every discrete-time points when calculating its corresponding self-excited force (Zhang and Chen 2011). In order to speed up the calculation and save the computational memory, by utilizing the principle of integration by parts and the nonlinear dynamic time-history analysis method, the integral sequence in Eq. (16) is converted into a recursive formula for calculation. Taking $F_{M\alpha}$ the torsional transfer function as an example, at moment t_i, we assume

$$R=\frac{d_kU}{B} \tag{18}$$

$$Z_i=\int_0^{t_i}e^{-R(t_i-\tau)}\dot{\alpha}(\tau)\mathrm{d}\tau \tag{19}$$

Thus, at moment t_{i+1}=(t_i+Δt), by using the method of integration by parts, we have

$$\begin{aligned}Z_{i+1}&=\int_0^{t_i+\Delta t}e^{-R(t_i+\Delta t-\tau)}\dot{\alpha}(\tau)\mathrm{d}\tau\\&=\int_0^{t_i}e^{-R(t_i+\Delta t-\tau)}\dot{\alpha}(\tau)\mathrm{d}\tau+\int_{t_i}^{t_i+\Delta t}e^{-R(t_i+\Delta t-\tau)}\dot{\alpha}(\tau)\mathrm{d}\tau\\&=Z_ie^{-R\Delta t}+\int_{t_i}^{t_i+\Delta t}e^{-R(t_i+\Delta t-\tau)}\dot{\alpha}(\tau)\mathrm{d}\tau\\&=Z_ie^{-R\Delta t}+\frac{1}{R}\left[\dot{\alpha}(t_i+\Delta t)-\dot{\alpha}(t_i)e^{-R\Delta t}\right]\\&\quad-\frac{1}{R}\int_{t_i}^{t_i+\Delta t}e^{-R(t_i+\Delta t-\tau)}\ddot{\alpha}(\tau)\mathrm{d}\tau\end{aligned} \tag{20}$$

Based on the constant-average-acceleration method, which is one of Newmark-β methods, we substitute $\ddot{\alpha}(\tau)=\frac{\ddot{\alpha}(t_i)+\ddot{\alpha}(t_i+\Delta t)}{2}$ into Eq. (20) and then get the recursive expression for torsional transfer function $F_{M\alpha}$, shown in Eq. (21). The recursive expressions for the rest functions are similar to $F_{M\alpha}$.

$$\begin{aligned}Z_{i+1}&=Z_ie^{-R\Delta t}+\frac{1}{R}\left[\dot{\alpha}(t_i+\Delta t)-\dot{\alpha}(t_i)e^{-R\Delta t}\right]\\&\quad-\frac{1}{R^2}\frac{\ddot{\alpha}(t_i)+\ddot{\alpha}(t_i+\Delta t)}{2}\left(1-e^{-R\Delta t}\right)\end{aligned} \tag{21}$$

4. Coupling property of dynamic equilibrium equations

Assuming that the displacement, velocity, acceleration and self-excited force at moment t_i are $x(t_i)$, $\dot{x}(t_i)$, $\ddot{x}(t_i)$ and $F(t_i)$, respectively; and at the moment t_{i+1}(=t_i+Δt), these four elements are $x(t_i+\Delta t)$, $\dot{x}(t_i+\Delta t)$, $\ddot{x}(t_i+\Delta t)$ and $F(t_i+\Delta t)$, then the equations of motion at moment t_i and t_{i+1} can be written as

$$[M]\{\ddot{x}(t_i)\}+[C]\{\dot{x}(t_i)\}+[K]\{x(t_i)\}=\{F(t_i)\} \tag{22}$$

$$\begin{aligned}&[M]\{\ddot{x}(t_i+\Delta t)\}+[C]\{\dot{x}(t_i+\Delta t)\}+[K]\{x(t_i+\Delta t)\}\\&=\{F(t_i+\Delta t)\}\end{aligned} \tag{23}$$

where [M], [C] and [K] refer to mass, damping, and stiffness matrices, respectively.

Based on the recursive formulas of self-excited force, it is necessary to apply the unsteady aerodynamic force in each load step when using ANSYS to calculate the self-excited vibration response. Since the force at moment t_{i+1} is associated with the state of motion (namely displacement, velocity and acceleration) at that moment, we can say that

only by obtaining the state of motion can we figure out the self-excited force at the moment accurately, but without the self-excited force of the moment, it is also difficult to obtain the state of motion. In other words, $F(t_i+\Delta t)$ is the function of the state of motion, $x(t_i+\Delta t)$, $\dot{x}(t_i+\Delta t)$ and $\ddot{x}(t_i+\Delta t)$, thus the relationship between the force and the state of motion at moment t_{i+1} can be defined by coupled-implicit equation. Even under the premise that the self-excited force and the state of motion in Eq. (22) are already known, the self-excited force and the state of motion in Eq. (23) are still difficult to solve directly. This paper puts forward a coupled-implicit equation method to solve Eq. (23) using ANSYS, which is a restart iterative method, to solve the accurate state of motion at moment t_{i+1} based on the concept of iteration and ANSYS restart technique.

5. Solving dynamic equilibrium equations by using restart iterative method

The overall idea is as follows. First, the state of motion at a certain moment is solved through iteration and then used to calculate the self-excited force of bridge deck. Then the self-excited force is acted on bridge deck to further iteratively solve the state of motion at next moment. The time is extended according to the pre-set time step, until the required time-history response is obtained. During this process, ANSYS restart technique, referred to as restart iterative method in this paper, is adopted to iteratively calculate the accurate vibration state at each time step. The advantage of this restart technique is obvious. When iterating between moments t_i and t_{i+1}, the moment t_i would always be the starting time. Every iteration can return to the same starting time, which would not cause time loss, thereby considering the time integration effects more accurately and efficiently.

It is assumed that the state of motion and self-excited force at moment t_i are both exact solutions, and then Eq. (22) is satisfied. When calculating the state of motion at moment t_{i+1}, it is firstly assumed that $F_1(t_i+\Delta t) = F(t_i)$. By substituting it into Eq. (23), we can get the state of motion $x_1(t_i+\Delta t)$, $\dot{x}_1(t_i+\Delta t)$ and $\ddot{x}_1(t_i+\Delta t)$ at moment t_{i+1}. However, in real situations, $F_1(t_i+\Delta t)$ and $F(t_i)$ are not equivalent, thus $F_2(t_i+\Delta t)$ calculated via the state of motion $x_1(t_i+\Delta t)$, $\dot{x}_1(t_i+\Delta t)$ and $\ddot{x}_1(t_i+\Delta t)$ is not equivalent to $F_1(t_i+\Delta t)$. We need to substitute $F_2(t_i+\Delta t)$ into Eq. (23) for calculation and repeat in sequence until both the state of motion $x_j(t_i+\Delta t)$, $\dot{x}_j(t_i+\Delta t)$, $\ddot{x}_j(t_i+\Delta t)$ of the j^{th} iteration and $x_{j+1}(t_i+\Delta t)$, $\dot{x}_{j+1}(t_i+\Delta t)$, $\ddot{x}_{j+1}(t_i+\Delta t)$ of the $j+1^{\text{th}}$ iteration meet certain requirements, and then we can obtain the real state of motion and self-excited force at moment t_{i+1}. The iteration error is controlled by Euclidean norm, with equations as follows

$$\left\{\frac{\sum_{k=1}^{Na}\left[x_{j+1,k}(t_i+\Delta t)-x_{j,k}(t_i+\Delta t)\right]^2}{\sum_{k=1}^{Na}\left[x_{j,k}(t_i+\Delta t)\right]^2}\right\}^{1/2} \le \varepsilon_1 \tag{24a}$$

$$\left\{\frac{\sum_{k=1}^{Na}\left[\dot{x}_{j+1,k}(t_i+\Delta t)-\dot{x}_{j,k}(t_i+\Delta t)\right]^2}{\sum_{k=1}^{Na}\left[\dot{x}_{j,k}(t_i+\Delta t)\right]^2}\right\}^{1/2} \le \varepsilon_2 \tag{24b}$$

$$\left\{\frac{\sum_{k=1}^{Na}\left[\ddot{x}_{j+1,k}(t_i+\Delta t)-\ddot{x}_{j,k}(t_i+\Delta t)\right]^2}{\sum_{k=1}^{Na}\left[\ddot{x}_{j,k}(t_i+\Delta t)\right]^2}\right\}^{1/2} \le \varepsilon_3 \tag{24c}$$

where $x_{j,k}$, $\dot{x}_{j,k}$ and $\ddot{x}_{j,k}$ are the calculated displacement, velocity and acceleration of the j^{th} iteration at node k, respectively; Na is the total number of nodes that need self-excited force to be acted on when calculating self-excited vibration of the structure; ε_1, ε_2 and ε_3 are tolerant Euclidean norm error limit for displacement, velocity and acceleration, respectively. Vertical and torsional state of motion should be calculated in Eq. (24) simultaneously.

The specific calculation steps are as follows:

① Suppose $F_1(t_i+\Delta t) = F(t_i)$ at moment t_{i+1};

② Calculate $x_j(t_i+\Delta t)$, $\dot{x}_j(t_i+\Delta t)$ and $\ddot{x}_j(t_i+\Delta t)$ at moment t_{i+1} using Eq. (23), and then calculate $F_{j+1}(t_i+\Delta t)$ using Eq. (17) of self-excited force;

③ Get back to the equilibrium state of moment t_i by using restart technique, then recalculate $x_{j+1}(t_i+\Delta t)$, $\dot{x}_{j+1}(t_i+\Delta t)$ and $\ddot{x}_{j+1}(t_i+\Delta t)$ at moment t_{i+1} with the newly-obtained self-excited force;

④ Determine whether the two calculation results of moment t_{i+1} satisfy the Eq. (24). If satisfied, turn to Step ⑤, otherwise, $j=j+1$, and calculate $F_{j+1}(t_i+\Delta t)$ using Eq. (17) of self-excited force, then turn to Step ③;

⑤ Extend the time according to pre-set time step Δt and repeat Steps ①~④ until total required time are calculated after the state of motion and self-excited force at moment t_{i+1} are obtained.

Due to the time integration effects in time domain solution, it is necessary to guarantee the invariance of the starting equilibrium state when iterating at time steps. In other words, every iteration should start from the equilibrium state of moment t_i when solving the state of motion at moment t_{i+1}. This requirement can be achieved by the restart technique in ANSYS. In transient analysis, restart analysis allows extra time-history analysis to be added at any time step and to return to the equilibrium state of any previous moment defined by time step from present moment without making previous calculating results invalid. Thus, by returning from the equilibrium state of moment t_{i+1} to that of moment t_i, countless times of calculation of time integral would be theoretically possible.

And every process of returning from moment t_{i+1} to moment t_i is regarded as an extra iterative process. The state of motion for each iteration would be saved alternatively in temporary array *ckport* and recorded array *nvexport*, and then values corresponding to these two arrays would be verified by the Euclidean norm as shown in Eq. (24). The calculation of next moment would not start until the

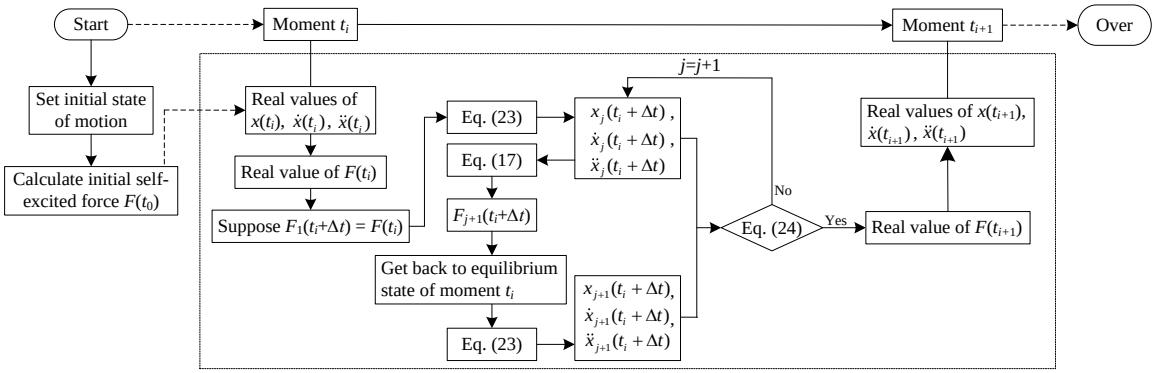

Fig. 1 Solution procedure of the restart iterative method

Fig. 2 The Maanshan Bridge

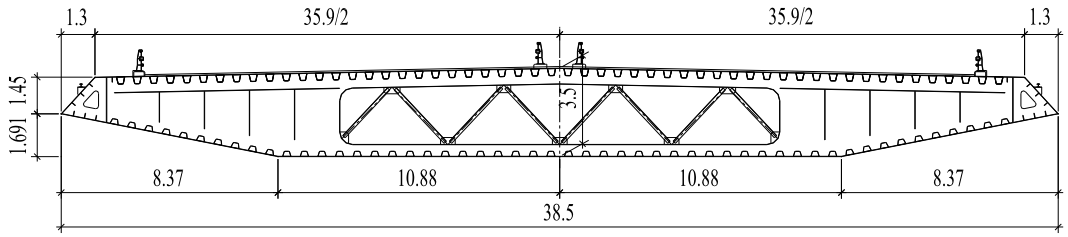

Fig. 3 Cross-section of the Maanshan Bridge's deck (unit: m)

required error tolerance is satisfied. The procedure of restart iterative method is shown in Fig. 1. The condition for onset of flutter instability becomes that, at a certain wind velocity, the amplitude of vibration is invariant with time.

6. Engineering example

The Maanshan Bridge across the Yangtze River in Anhui Province, China, is taken as an example to verify the applicability of the proposed method. This bridge, spanned as 360 m+2×1080 m+360 m, is a suspension bridge with three 176m high pylons of frame-structure, as shown in Fig. 2. The heights of the middle and side towers above the deck are 128 m and 143 m, respectively. As shown in Fig. 3, the deck cross section is an aerodynamically streamlined closed box steel deck 38.5 m wide and 3.5 m high. The lower crossbeam of the middle pylon is through the deck, making the deck fixed to the middle pylon. There are two one-way longitudinal movable supports under the deck on the lower crossbeam of each side tower; lateral wind-resistant supports are set between the deck and the columns of side towers. The two cables and all hangers are made of high tensile galvanized parallel wire bundles. The sag-to-span ratio of the main cable in two main spans is 1/9. The distance between the two cables is 35 m. The spacing between two adjacent hangers is 16.0 m. Material and geometrical features of main members are available in the literature (Zhang and Ge 2011).

As shown in Fig. 4, the bridge is simulated by using a three-dimensional finite element model in ANSYS.

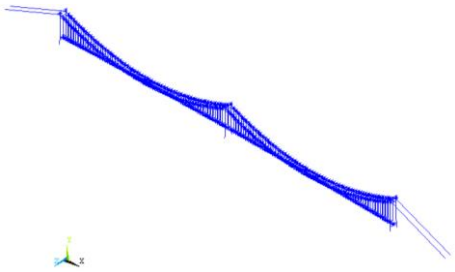

Fig. 4 Finite element model of the Maanshan Bridge

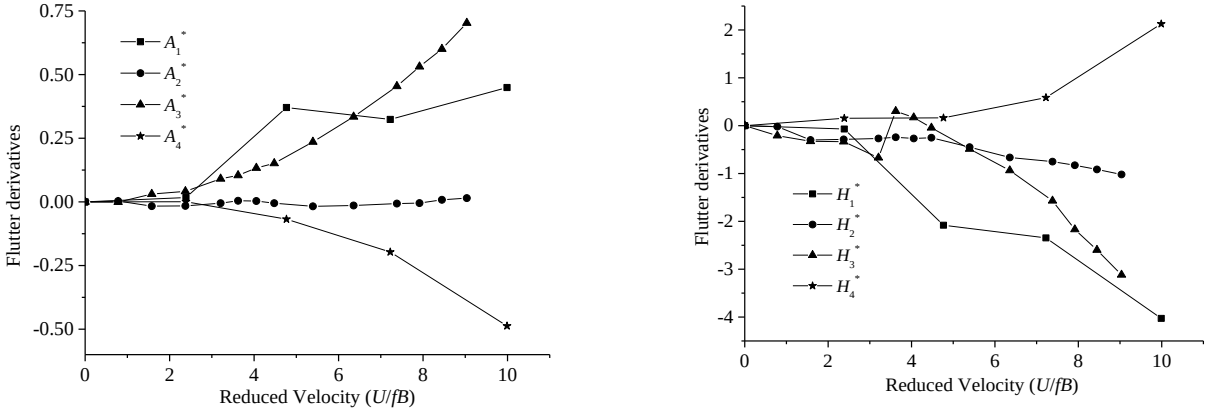

Fig. 5 The experimental flutter derivatives

Table 1 Parameters of impulse response functions

Component	C_1	C_2	C_3	C_4	d_3	d_4
L_h	0.9117	-25.4943	-8031.42	8574.017	10.5212	10.9047
L_α	80.3378	-0.5286	-818.725	738.1682	0.0855	0.0951
M_h	-0.0871	0.0811	-151.6058	152.3453	1.2571	1.2634
M_α	-4.0295	-0.0164	-7.4508	11.7910	0.0725	0.0465

Table 2 Flutter results

Result	Present procedure	Wind tunnel test (Ge *et al*. 2009)	Full-mode method (Zhang and Ge 2011)
Critical flutter wind velocity (m/s)	76.0	76.3	76.1
Flutter frequency (Hz)	0.2386	0.2341	0.2395

Three-dimensional beam elements are adopted to model three pylons. The cables and suspenders are modeled by three-dimensional link elements accounting for geometric nonlinearity due to cable sag. The bridge deck is represented by a single beam and the cross-section properties of the bridge deck are assigned to the beam as equivalent properties. The connections between bridge components and the supports of the bridge are properly modeled. According to the results of dynamic finite-element analysis, natural frequencies of the first vertical bending mode and torsional mode are 0.0843Hz and 0.2675Hz, respectively.

As illustrated in Fig. 5, the flutter derivatives of deck section under the wind attack angle of 0° have been experimentally measured from sectional-model tests in wind tunnel (Zhang and Ge 2011). Table 1 gives out the identified parameters of impulse response functions. The flutter derivatives obtained considering the impulse function parameters are compared with the experimental ones in Fig. 6.

Having assumed structural damping as 0.5%, time-domain flutter analysis of the Maanshan Bridge was conducted by using the method proposed in this paper. The pre-set time step is 0.1s. The response time histories of deck at the mid-point of a main span under different wind

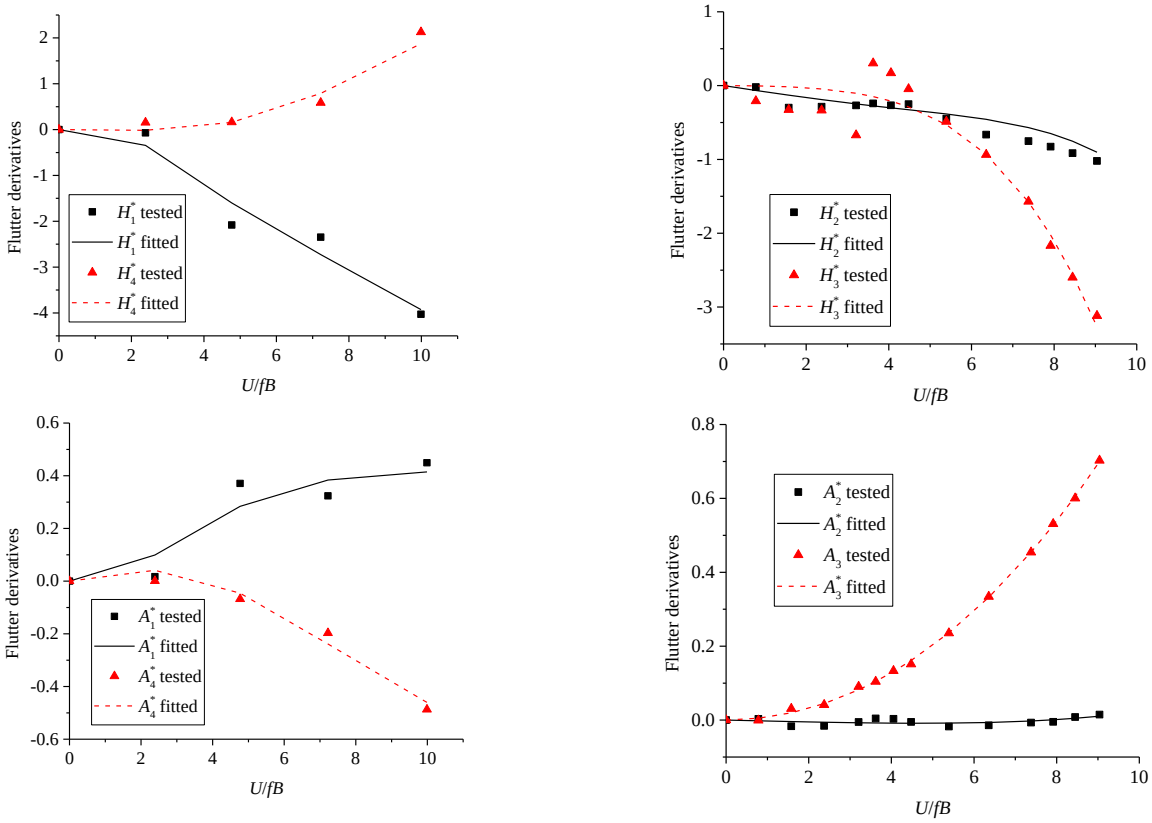

Fig. 6 Comparison of fitted flutter derivatives with those originally tested

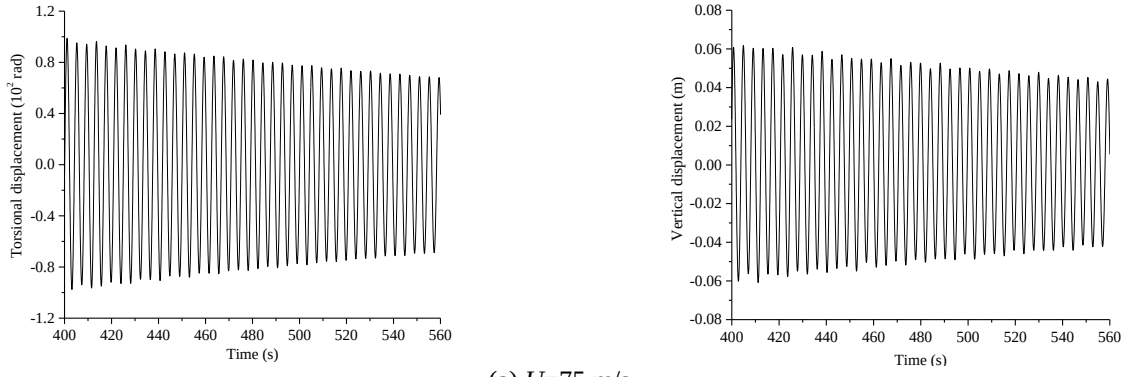

(a) U=75 m/s

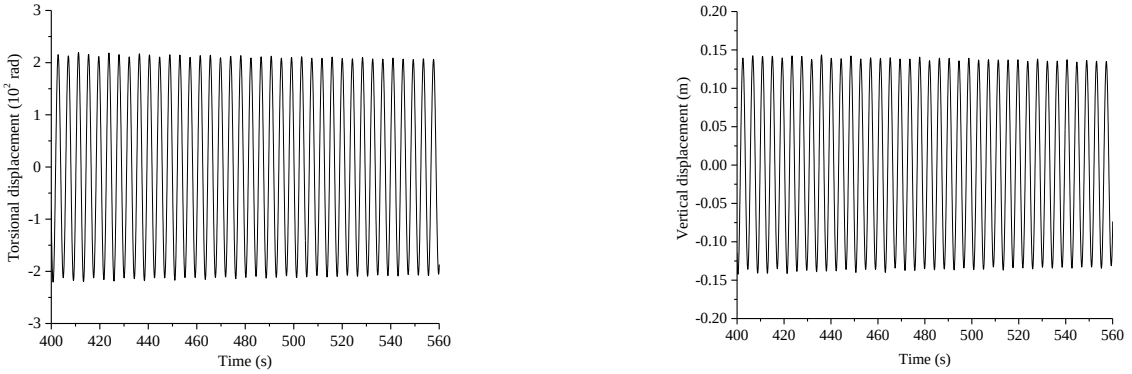

(b) U=76.0 m/s

Continued-

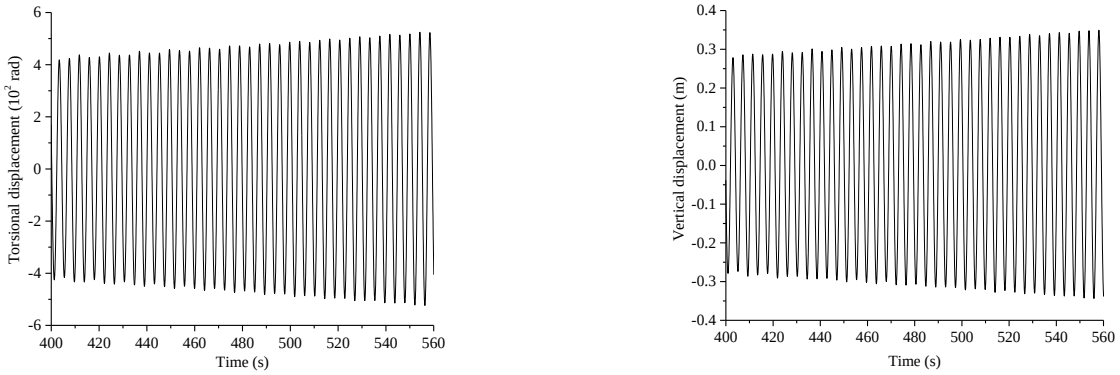

(c) U=76.5 m/s

Fig. 7 Time-domain response of deck at mid-point

velocities are obtained and shown in Fig. 7. It is recorded that the system is dynamically stable when the wind velocity is lower than the critical value and becomes dynamically unstable when the wind velocity is greater than the critical value. A good agreement between the critical flutter wind velocities obtained by the present procedure, wind tunnel test (Ge *et al*. 2009) and Full-mode flutter analysis (Zhang and Ge 2011) is observed in Table 2, so is the flutter frequency.

Typically, 5~10 iterations were required in the calculations of the self-excited forces at a certain moment. The full method for the transient analysis in ANSYS was used to solve the dynamic equation of the system. And the corresponding command is "TRNOPT, FULL". It took about 30 minutes to calculate a 100s time-history of the response at a certain wind speed using an ordinary personal computer.

7. Conclusions

This paper gives recursive expressions of calculating self-excited force for bridge deck based on impulse function of self-excited force, and puts forward a restart iterative method for time-domain analysis of bridges to be applied in solving flutter critical wind velocity based on ANSYS restart technique.

The numerical example of suspension bridge with flat steel box girder has proven that the flutter critical wind velocity and flutter frequency obtained by restart iterative method agree well with the results of both wind tunnel test and full-mode flutter analysis.

The restart iterative method of calculating flutter response proposed in this paper avoids frequency-targeted iteration and reflects vibration response of all participating modes, thus it can be further applied to the calculation of self-excited force in time-domain buffeting analysis for bridges.

Acknowledgments

The research described in this paper was financially supported by the National Science Foundation of China (No. 51678148), the Natural Science Foundation of Jiangsu Province (No. BK20181277) and the National Key R&D Program of China (No. 2017YFC0806009), which are gratefully acknowledged.

References

Agar, T.J.A. (1989), "Aerodynamic flutter analysis of suspension bridges by a modal technique", *Eng. Struct.*, **11**(2), 75-82.

Caracoglia, L. and Jones, N.P. (2003), "Time domain vs frequency domain characterization of aeroelastic forces for bridge deck sections", *J. Wind Eng. Ind. Aerod.*, **91**(3), 371-402.

Chen, Z.Q., Han, Y., Hua, X.G. and Luo, Y.Z. (2009), "Investigation on influence factors of buffeting response of bridges and its aeroelastic model verification for Xiaoguan Bridge", *Eng. Struct.*, **31**(2), 417-431.

Ding, Q.S. (2001), "Refinement of coupled flutter and buffeting analysis for long-span bridges", Ph.D. Dissertation; Tongji University, Shanghai, P.R. China (in Chinese).

Ding, Q.S., Chen, A.R. and Xiang, H.F. (2002), "Coupled flutter analysis of long-span bridges by multimode and fullorder approaches", *J. Wind Eng. Ind. Aerod.*, **90**(12-15), 1981-1993.

Dung, N. N., Miyata, T., Yamada, H. and Minh, N.N. (1998), "Flutter responses in long span bridges with wind induced displacement by the mode tracing method", *J. Wind Eng. Ind. Aerod.*, **77-78**, 367-379.

Ge, Y.J. and Tanaka, H. (2000), "Aerodynamic analysis of cable-supported bridge by multi-mode and full-mode approaches", *J. Wind Eng. Ind. Aerod.*, **86**(2-3), 123-153.

Ge, Y.J., Xu, L.S., Zhang, W.M. and Zhou, Z.Y. (2009), "Dynamic and aerodynamic characteristics of new suspension bridges with double main spans", *Proceedings of the 7th Asia-Pacific Conference on Wind Engineering*, Taipei, Taiwan.

Han, Y., Liu, S.Q., Cai, C.S. and Li, C.G. (2015a), "Flutter stability of a long-span suspension bridge during erection", *Wind Struct.*, **21**(1), 41-61.

Han, Y., Liu, S.Q., Cai, C.S., Zhang, J.R. Chen, S.R. and He, X.H., (2015b), "The influence of vehicles on the flutter stability of a long-span suspension bridge", *Wind Struct.*, **20**(2), 275-292.

Hua, X.G. and Chen, Z.Q. (2008), "Full-order and multimode flutter analysis using ANSYS", *Finite Elem. Anal. Des.*, **44**(9-10), 537-551.

Hua, X.G., Chen, Z.Q., Ni, Y.Q. and Ko, J.M. (2007), "Flutter analysis of long-span bridges using ANSYS", *Wind Struct.*, **10**(1), 61-82.

Jain, A., Jones, N.P. and Scanlan, R. H. (1996), "Coupled flutter and buffeting analysis of long-span bridges", *J. Struct. Eng.* -

ASCE, **122**(7), 716-725.
Katsuchi, H., Jones, N.P. and Scanlan, R.H. (1999), "Multimode coupled flutter and buffeting analysis of the Akashi-Kaikyo Bridge", *J. Struct. Eng. - ASCE*, **125**(1), 60-70.
Katsuchi, H., Jones, N.P., Scanlan, R.H. and Akiyama, H. (1998), "Multi-mode flutter and buffeting analysis of the Akashi-Kaikyo bridge", *J. Wind Eng. Ind. Aerod*., **77-78**, 431-441.
Li, Q.C. and Lin, Y.K. (1995), "New Stochastic theory for bridge stability in turbulent flow II", *J. Eng. Mech.*, **121**(1), 102-116.
Lin, Y.K. and Li, Q.C. (1993), "New Stochastic theory for bridge stability in turbulent flow", *J. Eng. Mech.*, **119**(1), 113-128.
Miyata, T. and Yamada, H. (1990), "Coupled flutter estimate of a suspension bridge", *J. Wind Eng. Ind. Aerod.*, **33**(1-2), 341-348.
Namini, A., Albrecht, P. and Bosch, H. (1992), "Finite element-based flutter analysis of cable-suspended bridges", *J. Struct. Eng.*, **118**(6), 1509-1526.
Scanlan, R.H. (1978), "Action of flexible bridges under wind, 1: flutter theory", *J. Sound Vib.*, 60(2), 187-199.
Starossek, U. (1998), "Complex notation in flutter analysis", *J. Struct. Eng.*, **124**(8), 975-977.
Tanaka, H., Yamamura, N. and Tatsumi, M. (1992), "Coupled mode flutter analysis using flutter derivatives", *J. Wind Eng. Ind. Aerod.*, **42**(1-3), 1279-1290.
Tang, H.J., Li, Y.L. and Shum, K.M. (2018), "Flutter performance of long-span suspension bridges under non-uniform inflow", *Adv. Struct. Eng.*, **21**(2), 201-213.
Wang, H., Chen, C.C., Xing, C.X., Li, A.Q. (2014a), "Influence of structural parameters on dynamic characteristics and wind-induced buffeting responses of a super-long-span cable-stayed bridge", *Earthq. Eng. Eng. Vib.*, **13**(3), 389-399.
Wang, H., Tao, T.Y., Zhou, R., Hua, X.G. and Kareem, A. (2014b), "Parameter sensitivity study on flutter stability of a long-span triple-tower suspension bridge", *J. Wind Eng. Ind. Aerod.*, **128** (5), 12-21.
Yang, D.C., Ge, Y.J., Xiang, H.F. and Ma, Z.G.J. (2011), "3D flutter analysis of cable supported bridges including aeroelastic effects of cables", *Adv. Struct. Eng.*, **14**(6), 1129-1147.
Zhang, W.M., Ge, Y.J. and Levitan, M.L. (2011), "Aerodynamic flutter analysis of a new suspension bridge with double main spans", *Wind Struct.*, **14**(3), 187-208.
Zhang, Z.T., Chen, Z.Q., Cai, Y.Y. and Ge, Y.J. (2011), "Indicial functions for bridge aeroelastic forces and time-domain flutter analysis", *J. Bridge Eng.*, **16**(4), 546-557.

AD